Tungsten oxide proton conducting films for low-voltage transparent oxide-based thin-film transistors

Hongliang Zhang, Qing Wan, Changjin Wan, Guodong Wu, and Liqiang Zhu

Related Articles

Additional information on Appl. Phys. Lett.

Tungsten oxide proton conducting films for low-voltage transparent oxide-based thin-film transistors

Hongliang Zhang, Qing Wan,[a] Changjin Wan, Guodong Wu, and Liqiang Zhu
Ningbo Institute of Material Technology and Engineering, Chinese Academy of Sciences,
Ningbo 315201, People's Republic of China

Tungsten oxide (WO_x) electrolyte films deposited by reactive magnetron sputtering showed a high room temperature proton conductivity of 1.38×10^{-4} S/cm with a relative humidity of 60%. Low-voltage transparent W-doped indium-zinc-oxide thin-film transistors gated by WO_x-based electrolytes were self-assembled on glass substrates by one mask diffraction method. Enhancement mode operation with a large current on/off ratio of 4.7×10^6, a low subthreshold swing of 108 mV/decade, and a high field-effect mobility 42.6 cm^2/V s was realized. Our results demonstrated that WO_x-based proton conducting films were promising gate dielectric candidates for portable low-voltage oxide-based devices. © 2013 American Institute of Physics. [http://dx.doi.org/10.1063/1.4791673]

An interesting feature of proton-conducting or ion-conducting electrolytes is their ability to form so-called electric-double-layer (EDL) capacitors.[1] For low-cost portable application, organic thin-film transistors (TFTs) gated by organic proton or ion conductors have been widely investigated.[1–5] In such organic TFTs, low-voltage operation is due to the formation of large EDL capacitance at the electrolyte/gate electrode and the electrolyte/channel interfaces. For example, 1.0 V operation of organic TFTs gated by a proton conducting polyelectrolytes with a high specific capacitance of $\geqq 10\,\mu$F/cm^2 at 100 Hz was reported by Herlogsson *et al.*[1] Crispin *et al.* investigated the relative humidity (RH) dependent polarization mechanism and interfacial EDL capacitor formation at low frequency in such organic proton conductor in detail.[2] Tungsten oxide (WO_x) was reported to be a good inorganic proton conductor.[6] For example, an aqueous proton conducting solid electrolyte WO_x has been reported to show a high proton conductivity of 7.0×10^{-3} S/cm at 150 °C under saturated water vapor pressure.[7] WO_x films with a very high resistivity of $2.4 \times 10^{11}\,\Omega$ cm were deposited by radio frequency (RF) reactive magnetron sputtering.[8] Sputtered WO_x film was a high-k insulator for ion-sensitive field-effect transistors fabrication.[9] Recently, low-voltage (2.0 V) ZnO-based TFTs gated by WO_x high-k gate dielectric film were reported, but proton conducting properties of the WO_x film was not investigated.[10]

At the same time, modulation of the threshold voltage and operation mode of oxide-based TFTs is of particularly high importance for realization of integrated circuits and relevant applications in chemical and biological sensors. In our previous work, it was demonstrated that self-assembled TFTs with indium-zinc-oxide (IZO) channel and source/drain electrodes usually work in depletion mode because of the high concentration electron in IZO film. W-doping can distinctly reduce the electron concentration of IZO film, which makes it possible for IZO-based TFTs operate in enhancement mode.[11,12] In this letter, we found that WO_x film deposited at room-temperature (RT) was a proton conductor with a RT proton conductivity of 1.38×10^{-4} S/cm. Self-assembled transparent W-doped IZO (WIZO) TFTs gated by WO_x proton conductor showed a low operation voltage of 1.8 V and a high field-effect mobility 42.6 cm^2/V s.

First, 550 nm-thick WO_x films were deposited on transparent conducing ITO glass and Si (100) substrates by RF (13.56 MHz) reactive magnetron sputtering using a metallic tungsten (99.995%) target at RT under a working pressure of 0.5 Pa. High pure Ar (99.995%) and O_2 (99.995%) were used as the reactive gases with a flow rate of 12/12 sccm. Then, patterned 200 nm-thick WIZO films for source/drain electrodes were deposited on the WO_x films by RF magnetron sputtering with a nickel shadow mask. WIZO films were deposited in 0.5 Pa pure Ar (99.995%) ambient by dual target RF magnetron co-sputtering of W and IZO (10 wt. % ZnO doped In$_2$O$_3$, 99.99%) at RT. The RF power density for WO_x films deposition is 7.5 W/cm^2. The power densities for W-doped IZO source/drain electrodes deposition are 5 W/cm^2 for IZO target, and 1.0 W/cm^2 for W target, respectively. Here, we should point out that a thin WIZO channel can be self-assembled between the source/drain electrodes due to the diffraction effect when the distance between the nickel shadow mask and substrate is $\sim$50 μm. If the distance was too small ($<$10 μm), the self-assembled channel would gradually disappear. If the distance is too large, the self-assembled channel would eventually become too thicker ($\geq$80 nm) for used as transistor channel layer. The channel width and length of the shadow mask are 1000 μm and 80 μm, respectively. The entire process of the device fabrication was performed at room temperature. Field-emission scanning electron microscopy (FE-SEM, Hitachi S-4800) and impedance analyzer (Solartron 1260) were employed for WO_x electrolyte film characterization. The electrical measurements of TFTs were carried out using a semiconductor parameter analyzer (Keithley 4200 SCS) at room temperature in dark with a RH of 60%. The transfer characteristics of the devices were measured at a voltage sweep rate of 30 mV/s.

Figure 1(a) shows the cross-section SEM image of the WO_x film deposited on Si (100) substrate, and the thickness

[a]Author to whom correspondence should be addressed. Electronic mail: wanqing@nimte.ac.cn. Tel./Fax: +86 574 8669 0355.
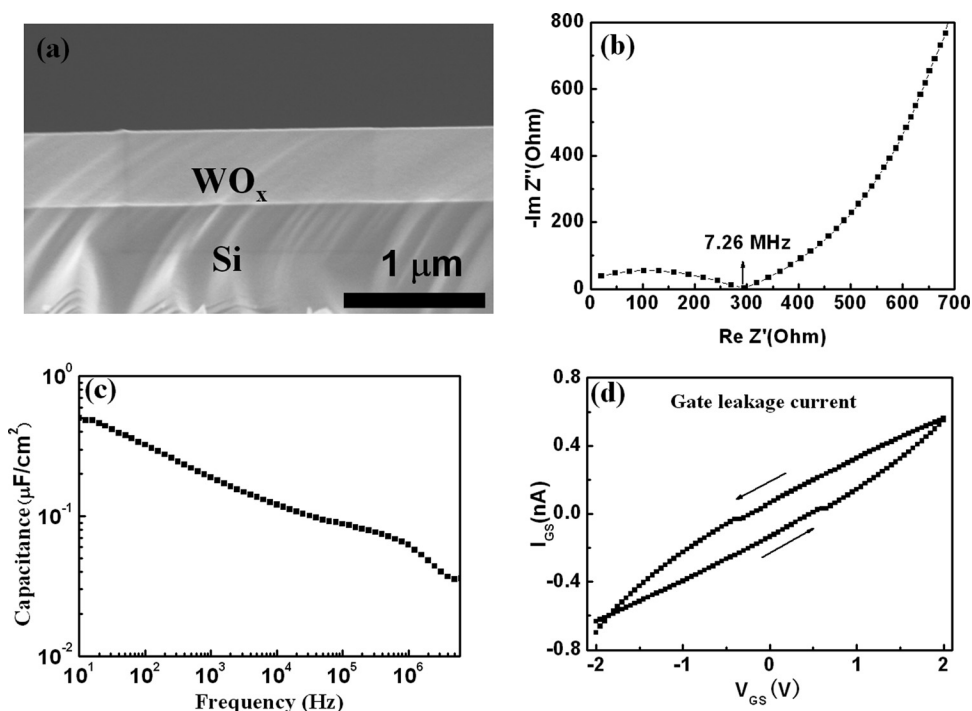
FIG. 1. (a) Cross-section SEM image of the WO_x film deposited on (100) Si substrate. (b) Typical Cole-Cole plot, (c) frequency dependent specific capacitance, and (d) gate leakage current of the WO_x film measured at 60% RH at room temperature with an ITO/WO_x/ITO sandwich test structure.

is estimated to be 550 nm. The RT proton conductivity of the WO_x film was determined from Cole-Cole plots by an AC method at 60% RH. The Cole-Cole plot consisted of a single semicircle and the proton conductivity was obtained from the intersecting point of the semicircle with the real axis, as shown in Fig. 1(b). The proton conductivity, σ, was calculated from R and pellet dimension, i.e., $\sigma = L/(R - R_0)A$,[13] where L, A, and R_0 are thickness of the WO_x film, electrode surface area and the rig short circuit resistance, respectively. The proton conductivity of WO_x electrolyte film is calculated to be 1.38×10^{-4} S/cm ($R_0 = 30$ Ω). The high proton conductivity indicates that absorbed water is favorable for proton conduction in WO_x film. Figure 1(c) shows the specific gate capacitance of the WO_x film in the frequency range of 10 Hz-6.0 MHz. The specific gate capacitance, C_i at low frequency (10 Hz) is estimated to be 0.5 μF/cm^2. The specific capacitance of 550-nm-thick WO_x dielectric should be 0.11 μF/cm^2 if a dielectric constant of 70 is adopted. This large difference is due to the electric-double-layer effect related to the proton conducting characteristic of WO_x. Transfer curves of oxide-based TFTs are measured at quasi-static condition. So, specific gate capacitance at low frequency should be used for field-effect mobility calculation, otherwise, the estimated mobility will be overestimated. In our work, in order to get true mobility, the specific gate capacitance at 10 Hz will be used. Similar to the results reported by Larsson *et al.*,[2] the capacitive behavior at low frequencies of WO_x-based proton conductor is associated with the formation of EDLs at WO_x solid electrolyte/IZO electrode interfaces. Fig. 1(d) shows the current leakage curve of the WO_x film in the bias voltage of ±2.0 V, and a low gate leakage current of less than 0.7 nA was obtained.

Figure 2(a) shows the schematic diagram of self-assembled WIZO-based TFTs gated by WO_x proton conducting film on transparent conducting glass substrate. Only one shadow mask is needed for IZO-based homojunction TFTs fabrication because patterned IZO channel can be

self-aligned between IZO-based source/drain electrodes simultaneously during one-step sputtering process. Here, we should point out that a proper mask-to-substrate distance must be chosen to precisely control the thickness and uniformity of the active channel. Here, the distance between the mask and substrate during deposition is about 50 μm. Figure 2(b) shows the optical transmission spectra of the W-doped IZO TFT arrays on an ITO glass substrate. The TFT arrays show an optical transmittance of $\geq$86% in the visible light
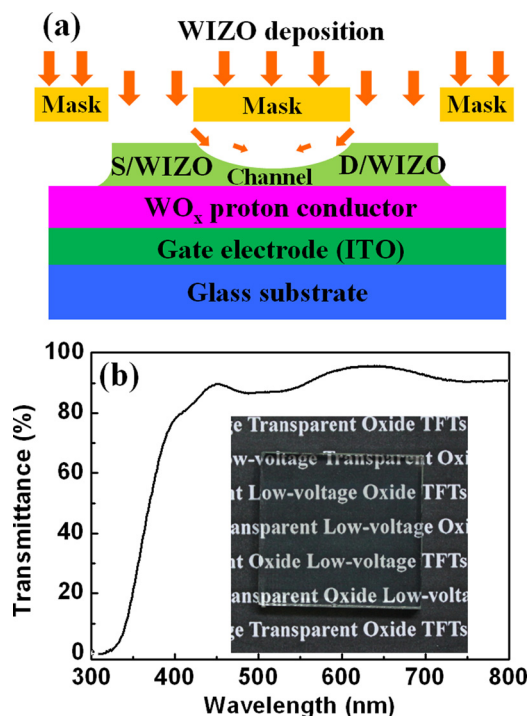

FIG. 2. (a) Schematic image of a WIZO-based TFT gated by WO_x proton conductor film self-assembled on glass substrate. (b) Optical transmission spectra of the entire TFT arrays on an ITO glass substrate. Inset: a picture of the TFT arrays placed on background text.

region. The inset in Fig. 2(b) shows a photograph of the WO_x TFT arrays placed on background text, indicating its highly transparent characteristics to visible light.

Figure 3(a) shows the output characteristics (I_{DS}–V_{DS}) of the transparent WIZO-based TFTs with V_{GS} varied from 1.1 to 1.7 V in 0.1 V steps. The curves exhibit good current saturation behaviors at high V_{DS} and linear characteristics of I_{DS} at low V_{DS}. Fig. 3(b) shows the corresponding transfer characteristics of the WIZO-based TFTs with $V_{DS} = 1.2$ V. Such TFT exhibits a high-performance with a large current on/off ratio of 4.7×10^6 and a small subthreshold swing of 108 mV/decade, respectively. A threshold voltage (V_{th}) of 1.0 V was calculated from the x-axis intercept of the square root of I_{DS}-versus-V_{GS} plot, indicating fully enhancement mode operation. It was reported that there were three approaches to shift the turn-on voltage and operation mode: (1) channel thickness variation, (2) intrinsic electron concentration of the channel, and (3) work function difference between the channel and gate electrode. Lorenz *et al.* realized the enhancement mode operation using Pt gate electrode with high work function of 5.65 eV.[14] In our experiment, in order to reduce the intrinsic electron concentration in IZO channel for fully enhancement mode operation, W-doping was adopted. The field-effect mobility (μ) in the saturation region ($V_{DS} > V_{GS} - V_{TH}$) can be derived from the following equation: $I_{DS} = (WC_i\mu/2L)(V_{GS} - V_{th})^2$, where $L = 80\,\mu m$ is the channel length, $W = 1000\,\mu m$ is the channel width, and C_i is the specific gate capacitance. Field-effect mobility was calculated to be as high as 42.6 cm^2/V s.
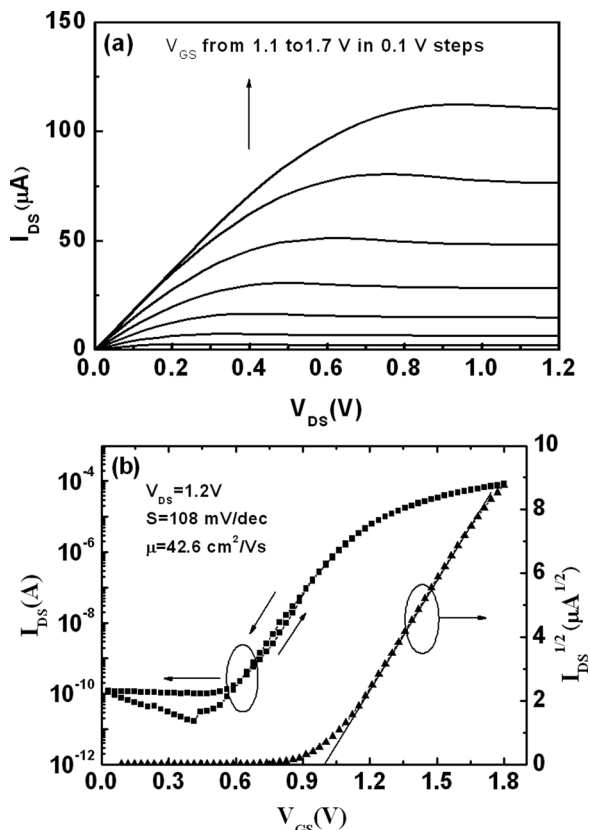

FIG. 3. Electrical characteristics of the WIZO-based TFTs gated by WO_x proton conducting film. (a) Output characteristics. V_{DS} was swept from 0 to 1.2 V at each V_{GS} varied from 1.1 to 1.7 V with 0.1 V steps. (b) Transfer characteristics at a fixed $V_{DS} = 1.2$ V.
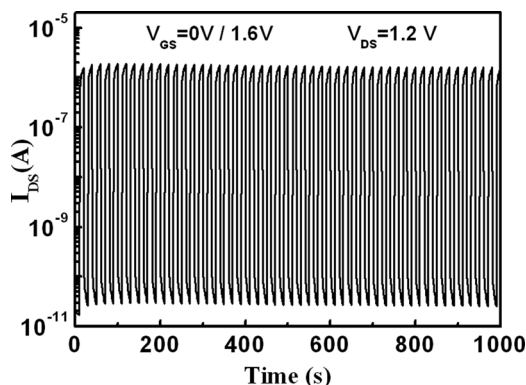

FIG. 4. Time response of the WIZO-based TFTs gated by WO_x proton conducting film to a pulsed square-shaped gate voltage with a pulsed amplitude of $V_+ = 1.6$ V and $V_- = 0$ V, showing a good reproducibility.

Figure 4 shows the transient response of the WIZO-based TFTs gated by WO_x proton conductor to a square-shaped V_{GS} with a pulsed amplitude of $V_+ = 1.6$ V and $V_- = 0$ V. The device exhibits an excellent reproducibility of current response to the repeatedly pulsed V_{GS}. This strongly suggests that no chemical doping or chemical reaction occurs at the WO_x/WIZO interface when the gate potential is biased, because if chemical doping or a chemical reaction had occurred, I_{DS} would not have returned to its original value after gate scanning. The stability of oxide-based TFTs remains as one of the crucial issues for practical applications. Improvement in the negative gate bias thermal stability of the TFTs can be achieved by post-annealing,[15–17] plasma treatment,[18] surface passivation,[19,20] etc. Moisture in ambient air has a significant impact on the stability of our WIZO-based TFTs gated by WO_x proton conducting films. The effect of moisture on the negative gate bias thermal stability of such TFTs will be further investigated in our future work.

The low-voltage operation mechanism of the WIZO-based TFTs gated by WO_x proton conducting electrolyte is explained as follows. When an electric potential is applied between the gate electrode and channel, mobile protons (H^+) in the WO_x-based proton conductor will move towards the oppositely charged electrodes to form interfacial EDLs as shown in Fig. 5(a). The EDL at WO_x/channel interface, regarded as a nanogap capacitor with a huge capacitance, can accumulate charges in the WIZO channel to a very high density level which is impossible for conventional gate dielectric. At the same time, the optical gaps of the WO_x and WIZO films were estimated to be 3.09 eV and 3.51 eV by means of optical transmission, respectively. The band gap of WIZO channel is wider than that of WO_x by 0.42 eV with the conduction band of the WIZO layer positioning above the conduction band of WO_x, as shown in Fig. 5(b). When no bias voltage is applied to the gate electrode, the potential difference between WIZO and WO_x results in the electron transfer from WIZO to WO_x, which induces the band bending-up of WIZO layer at the interface, i.e., the formation of the depletion region in WIZO. As a result, TFTs are normally turned off without gate voltage bias. When the gate is positively biased, an electron accumulation layer is formed in the W-doped IZO channel by the strong electrostatic modulation of the large EDL capacitance of WO_x-based solid
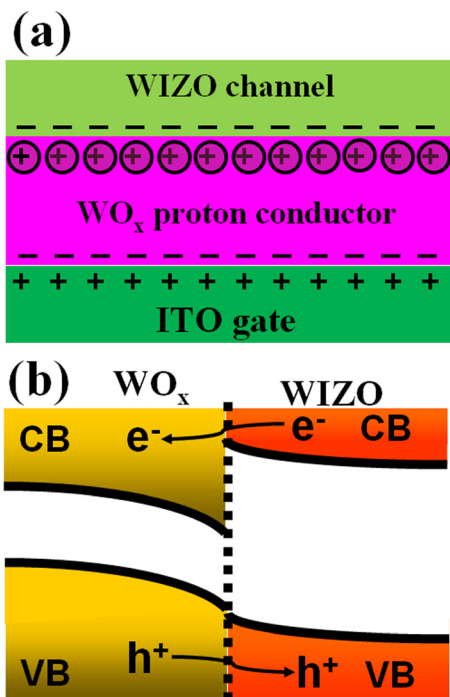
FIG. 5. (a) Schematic image of the EDL formation and electron accumulation with a positive gate bias stress. (b) Energy level diagram for WO_x/WIZO.

electrolyte. So, such TFTs gated by WO_x proton conducting electrolyte exhibit enhancement mode operation with a low operation voltage of 1.8 V. To confirm our explanation, we also performed Hall effect measurement. 30 nm-thick WIZO films deposited on WO_x/fused quartz substrate show a resistivity of 7.5 Ω cm, which is much higher than that of the WIZO films on fused quartz substrate without WO_x. In fact, Lorenz *et al.*[14] suggested that the WO_x dielectric gives rise to a reduced carrier concentration within the channel. The formation of a narrow layer of non-stoichiometric WO_x with n-type characteristics at the semiconductor-insulator interface may give rise to a band bending within the channel layer, which will reduce the electron concentration in the channel. Our experimental results are in good agreement with their reported results. So, electron depletion due to electron transfer from WIZO channel to WO_x proton conductor is another important reason for fully enhancement mode operation of such kind TFTs.

In summary, WO_x films deposited by RF sputtering at room temperature had a high proton conductivity of 1.38×10^{-4} S/cm at room temperature with a 60% RH.

Transparent low-voltage (1.8 V) WIZO-based TFTs gated by WO_x electrolyte films were self-assembled on ITO glass substrates by one mask diffraction method. High-performance with a large current on/off ratio of 4.7×10^6, a low subthreshold swing of 108 mV/decade, and a high field-effect mobility 42.6 cm^2/V s was obtained. Electron depletion of channel by W-doping and electron transfer from channel to WO_x gate dielectric were believed to be the reasons for fully enhancement mode operation. Such low-voltage transparent TFTs gated by WO_x proton conductor are very promising candidates for low-cost portable sensors.

[1]L. Herlogsson, X. Crispin, N. D. Robinson, M. Sandberg, O. J. Hagel, G. Gustafsson, and M. Berggren, Adv. Mater. **19**, 97 (2007).

[2]O. Larsson, E. Said, M. Berggren, and X. Crispin, Adv. Funct. Mater. **19**, 3334 (2009).

[3]N. Kaihovirta, H. Aarnio, C.-J. Wikman, C.-E. Wilén, and R. Österbacka, Adv. Funct. Mater. **20**, 2605 (2010).

[4]N. J. Kaihovirta, C.-J. Wikman, T. Mäkelä, C.-E. Wilén, and R. Österbacka, Adv. Mater. **21**, 2520 (2009).

[5]J. H. Cho, J. Lee, Y. He, B. S. Kim, T. P. Lodge, and C. D. Frisbie, Adv. Mater. **20**, 686 (2008).

[6]G. Orsini and V. Tricoli, J. Mater. Chem. **20**, 6299 (2010).

[7]Y. M. Li, M. Hibino, M. Miyayania, and T. Kudo, Solid State Ionics **134**, 271 (2000).

[8]H. Kaneko, S. Nishimoto, K. Miyake, and N. Suedomi, J. Appl. Phys. **59**, 2526 (1986).

[9]J. C. Chou and J. L. Chiang, Sens. Actuators B **62**, 81 (2000).

[10]M. Lorenz, H. von Wenckstern, and M. Grundmann, Adv Mater. **23**, 5383 (2011).

[11]B.-Y. Oh, J.-C. Park, Y.-J. Lee, S.-J. Cha, J.-H. Kim, K.-Y. Kim, T.-W. Kim, and G.-S. Heo, J. Solid State Chem. **184**, 2462 (2011).

[12]Y.-J. Lee, B.-W. Lim, J.-H. Kim, T.-W. Kim, B.-Y. Oh, G.-S. Heo, and K.-Y. Kim, J. Nanosci. Nanotechnol. **12**, 5604 (2012).

[13]Y. Jin, S. Qiao, J. C. D. da Costa, B. J. Wood, B. P. Ladewig, and G. Q. Lu, Adv. Funct. Mater. **17**, 3304 (2007).

[14]M. Lorenz, A. Reinhardt, H. von Wenckstern, and M. Grundmann, Appl. Phys. Lett. **101**, 183502 (2012).

[15]A. Suresh and J. F. Muth, Appl. Phys. Lett. **92**, 033502 (2008).

[16]R. B. M. Cross and M. M. De Souza, Appl. Phys. Lett. **89**, 263513 (2006).

[17]B. Ryu, H.-K. Noh, E.-A. Choi, and K. J. Chang, Appl. Phys. Lett. **97**, 022108 (2010).

[18]S. Yang, K. Hwan Ji, U. K. Kim, C. S. Hwang, S.-H. Ko Park, C.-S. Hwang, J. Jang, and J. K. Jeong, Appl. Phys. Lett. **99**, 102103 (2011).

[19]S. Yang, D.-H. Cho, M. K. Ryu, S.-H. K. Park, C.-S. Hwang, J. Jang, and J. K. Jeong, Appl. Phys. Lett. **96**, 213511 (2010).

[20]K.-H. Lee, J. S. Jung, K. S. Son, J. S. Park, T. S. Kim, R. Choi, J. K. Jeong, J.-Y. Kwon, B. Koo, and S. Lee, Appl. Phys. Lett. **95**, 232106 (2009).